Articles

Multicomponent Polyanions. 57. Large-Angle X-ray Scattering Study of Aqueous Molybdophenylphosphonate Solutions

Dan-Göran Lyxell,*,† Lage Pettersson,† and Ingmar Persson‡

Inorganic Chemistry Section, Department of Chemistry, Umeå University, SE-901 87 Umeå, Sweden, and Department of Chemistry, Swedish University of Agricultural Sciences, P.O. Box 7015, SE-750 07 Uppsala, Sweden

Received June 27, 2000

The radial distribution functions are calculated from large-angle X-ray scattering (LAXS) measurements for one concentrated aqueous molybdate/heptamolybdate solution and five aqueous molybdophenylphosphonate solutions (lithium chloride medium). Besides water and hydrated lithium, chloride, and molybdate ions, five species in all, having different nuclearities, are postulated to exist in the solutions, according to equilibrium studies using potentiometry and ^{31}P NMR spectroscopy. The structures of the three polymolybdate species $Mo_7O_{24}^{6-}$, $Mo_8O_{26}^{4-}$, and $(C_6H_5P)_2Mo_5O_{21}^{4-}$, for which the structures are determined crystallographically, are confirmed to exist also in aqueous solution. The principal structures of the remaining two complexes, $(C_6H_5P)Mo_6O_{21}(OH_2)_5^{2-}$ and $(C_6H_5P)Mo_7O_{25}(OH_2)^{4-}$, are elucidated with the use of structures of related species. Both anions have one group of four edge-sharing MoO_6 octahedra and another group of two MoO_6 octahedra connected by sharing corners, forming a bent unsymmetric six-membered ring, with the $C_6H_5PO_3$ group placed on the crowded side of the ring. In the former, the group of two MoO_6 octahedra is edge-shared, while in the latter, the group is face-shared, resulting in a ring small enough to tetrahedrally coordinate to the seventh molybdenum opposite the phenyl group.

Introduction

Hexavalent molybdenum and tungsten and pentavalent vanadium form a wide range of polyoxometalate complexes with a large variety of sizes, compositions, and structures in aqueous solution.[1] Many of these complexes have shown catalytic properties and have therefore been studied extensively.[2] The speciation of aqueous polyoxometalate systems has mainly been determined by potentiometric and NMR spectroscopic methods, and numerous structures have been determined by single-crystal X-ray techniques for solid phases precipitated from aqueous solutions. However, it has not been possible to crystallize all species postulated from equilibrium measurements. Furthermore, it cannot always be proven that the composition of a species present in aqueous solution and in the solid state are identical because, e.g., the degrees of hydration may differ. It is therefore important to perform structural studies in aqueous solution to obtain structural information for a species in the same medium as that in which the equilibrium studies were carried out.

The speciation of the molybdophenylphosphonate system was determined from a combination of potentiometric and ^{31}P NMR

data for dilute solutions where $C_{Mo} \leq 0.080$ mol·dm^{-3} (0.600 mol·dm^{-3} NaCl supporting electrolyte; 25 °C).[3] The equilibria of this system are written as

$$pH^+ + qMoO_4^{2-} + rC_6H_5PO_3^{2-} \rightleftharpoons$$
$$H_p(MoO_4)_q(C_6H_5PO_3)_r^{p-2q-2r}$$
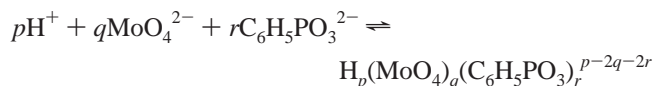
where the integers p, q, and r define the complexes formed. In the following, when we refer to nuclearities, the complexes will be designated as $Mo_q(PhP)_r$; for species in the proton series, the charge of the species will be given as well.

For the molybdophenylphosphonate system, only the Mo_5-$(PhP)_2$ species has been structurally characterized.[4] The proposed Mo_6PhP and Mo_7PhP species have not been structurally characterized, as it has not been possible to crystallize these complexes. To determine their structures and to verify the Mo_5-$(PhP)_2$ structure in aqueous solution, a series of large-angle X-ray scattering (LAXS) studies were carried out. LAXS studies require high concentrations to give reliable results, and $C_{Mo} = 1.50$ mol·dm^{-3} was chosen. The system was not sufficiently soluble for LAXS studies with sodium as the countercation, as used in the equilibrium studies.[3] Instead, lithium was used as the countercation because it allowed for sufficient solubility. The distribution diagrams, shown in Figure 1 (phenylphosphonate-containing species) and Figure 2 (molybdenum-containing species), were constructed using the equilibrium constants obtained in the previous speciation study.[3] ^{31}P NMR analyses of the concentrated solutions with LiCl as the supporting electrolyte, used in the structural studies, were found to be in

---

† Umeå University.

‡ Swedish University of Agricultural Sciences.

(1) Pope, M. T. *Heteropoly and Isopoly Oxometalates*; Springer-Verlag: New York, 1983.

(2) Pope, M. T.; Müller A. *Polyoxometalates*: *From Platonic Solids to Anti-Retroviral Activity*; Kluwer Academic Publishers: Dordrecht, The Netherlands, 1994; pp 255−335.

(3) Yagasaki, A.; Andersson, I.; Pettersson, L. *Inorg. Chem.* **1987**, *26*, 3926−3933.

(4) Lyxell, D.-G.; Strandberg, R. *Acta Crystallogr.*, *Sect. C* **1988**, *44*, 1535−1538.
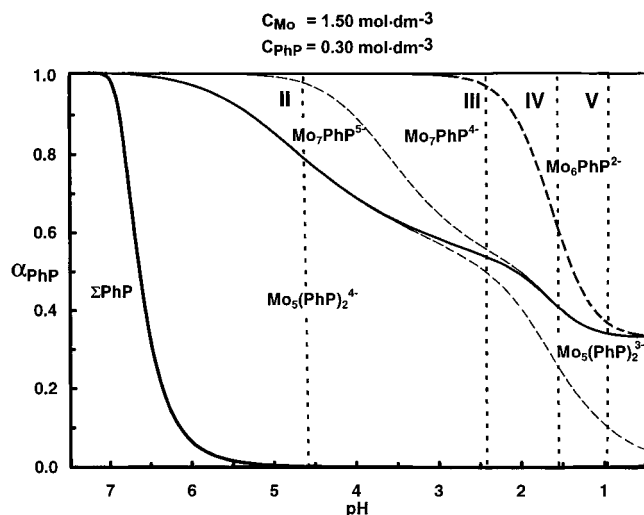
Figure 1. Cumulative distribution of phenylphosphonate-containing species, α_{PhP}, as a function of pH at Mo/PhP = 5. Each species is represented by an area, and its fraction is represented by the area's vertical height at that pH. Solid curves separate species that give different ^{31}P NMR resonances. Dashed curves separate species that cannot be differentiated because of rapid exchange on the NMR time scale. The vertical dashed lines indicate solutions used for LAXS measurements.
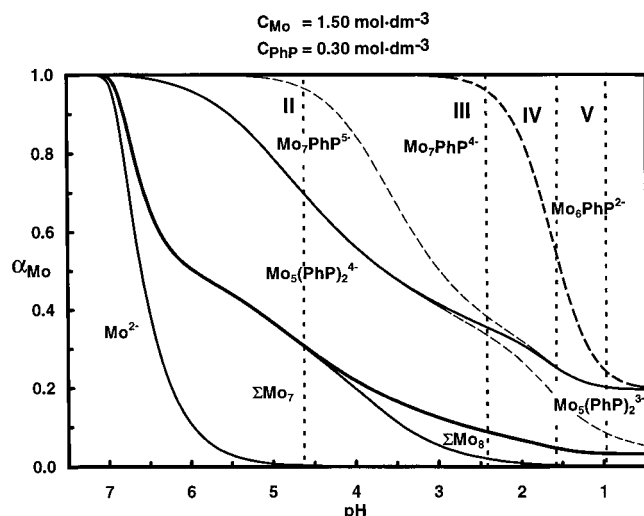

Figure 2. Cumulative distribution of molybdenum-containing species, α_{Mo}, as a function of pH at Mo/PhP = 5. The sum of the heptamolybdates and the sum of octamolybdates are shown.

Table 1. Compositions of Solutions I–VI[a]

| component | solution | | | | | |
	I	II	III	IV	V	VI
MoO_4^{2-}	1.500	1.500	1.500	1.500	1.500	1.500
$C_6H_5PO_3^{2-}$	0.600	0.300	0.300	0.300	0.300	0
Li^+	1.200	1.125	1.125	1.150	1.125	1.860
H^+	3.000	2.475	2.672	2.826	3.075	1.140
Cl^-	0	0	0.197	0.376	0.600	0
H_2O	48.97	51.30	50.35	50.12	49.40	52.53
pH	3.30	4.60	2.41	1.55	0.95	6.21
ρ	1.20	1.20	1.19	1.20	1.20	1.19
μ	10.111	10.087	10.115	10.154	10.280	10.053
V	1107.0	1107.0	1107.0	1107.0	1107.0	1107.0

[a] Concentrations are given in mol·dm^{-3}. ρ = density (g·cm^{-3}); μ = absorption coefficient (cm^{-1}); V = stoichiometric unit volume (Å^3).

the solid state and aqueous solutions. These studies showed identical structures in both phases for these three complexes.[5,6]

Experimental Section

Chemicals. Phenylphosphonic acid, $C_6H_5PO(OH)_2$ (Aldrich, 98%), molybdenum(VI) oxide, MoO_3 (E. Merck, 99.5%), lithium molybdate(VI), Li_2MoO_4 (Aldrich, 99%), and hydrochloric acid (E. Merck, p.a.) were used without further purification. Dilute hydrochloric acid was standardized against tris(hydroxymethyl)aminomethane (TRISMA base). Boiled distilled water was used in the preparation of all solutions.

Preparations of the Solutions. The solution of $Mo_5(PhP)_2$ (solution I), C_{Mo} = 1.50 mol·dm^{-3} (see Table 1), and two lithium molybdophenylphosphonate stock solutions, C_{Mo} = 2.0 mol·dm^{-3}, $C_{C_6H_5PO_3^{2-}}$ = 0.40 mol·dm^{-3}, C_{Li^+} = 1.5/2.0 mol·dm^{-3}, and C_{H^+} = 3.3 mol·dm^{-3}, were prepared from stoichiometric amounts of phenylphosphonic acid, molybdenum(VI) oxide, and lithium molybdate(VI) to which hydrochloric acid was added. Solutions II–V were prepared from the stock solutions by adding appropriate amounts of water and/or hydrochloric acid (Table 1). Since precipitation was observed after some days in solution V, the final addition of acid was made less than 24 h in advance of the LAXS measurements. No precipitation occurred during the LAXS data collection. Solution VI was prepared by mixing appropriate amounts of molybdenum(VI) oxide, lithium molybdate(VI), and water (Table 1).

Investigated Solutions. In total, six different solutions were investigated (Table 1). Four measurements were made on solutions with C_{Mo} = 1.50 mol·dm^{-3} and C_{PhP} = 0.30 mol·dm^{-3} at four different pH values (vertical dashed lines in the distribution diagrams shown in Figures 1 and 2). In the distribution diagram of Figure 1, only the phenylphosphonate-containing species are shown. Since, all molybdenum is not bound in MoPhP species, the diagram in Figure 2 is more relevant for the LAXS experiments. As seen in Figure 2, the molybdenum-containing species present in solutions II–V are isopolymolybdates ($Mo_7O_{24}^{n-}$, $Mo_8O_{26}^{n-}$) and heteropolymolybdates ($Mo_x(PhP)_y^{n-}$). All species, except Mo_6PhP, also undergo protonation, and the protonation series for hepta- and octamolybdates are indicated with summation signs (ΣMo_7 and ΣMo_8) in Figure 2. The charges are given for the phenylphosphonates (e.g., Mo_6PhP^{2-}). The thick solid line in Figure 2 separates the phenylphosphonate-containing species from the molybdate and isopolymolybdate species. The thin solid lines separate different species in each category, and the thick dashed line separates the Mo_7PhP and Mo_6PhP species.

Our strategy involves obtaining knowledge about the X-ray scattering features from the various contributors in the solution. The structure of $Mo_5(PhP)_2^{4-}$ in aqueous solution (solution I) was studied to confirm that the structure in the solid state was maintained in aqueous solution. The structures of the hydrated lithium and molybdate(VI) ions in aqueous solution were determined in a separate study.[7] Solution VI

very good agreement with the distribution diagram shown in Figure 1. The LAXS technique responds to all distances in a studied solution weighted by the number of distances and the number of electrons of the atoms involved. This means that, e.g., Mo···Mo and Mo···P distances are much easier to detect than distances between light atoms. This also means that a correct complex distribution of a studied solution is required to obtain a good fit between experimental data and the proposed model. LAXS studies on polyoxomolybdate complexes in aqueous solution were reported previously.[5,6] In the molybdate and molybdophosphate systems, the structures of the $Mo_7O_{24}^{6-}$, $Mo_8O_{26}^{4-}$, and $Mo_5P_2O_{23}^{6-}$ complexes were determined in both

(5) Johansson, G.; Pettersson, L.; Ingri, N. *Acta Chem. Scand.*, *Ser. A* **1974**, *28*, 1119−1128.
(6) Johansson, G.; Pettersson, L.; Ingri, N. *Acta Chem. Scand.*, *Ser. A* **1979**, *33*, 305−312.

(7) Persson, I.; Lyxell, D.-G.; Pettersson, L. Unpublished results.
(8) Sjöbom, K.; Hedman, B. *Acta Chem. Scand.* **1973**, *27*, 3673−3691.
(9) McCarron, E. M., III; Harlow, R. L. *Acta Crystallogr., Sect. C* **1984**, *40*, 1140−1141.

Table 2. Concentrations of the Complexes in the Solutions I−VI (mol·dm^{-3})

	solution					
complex	I	II	III	IV	V	VI[a]
$Mo_7O_{24}^{6-}$	0	0.0560	0	0	0	0.1425
$Mo_8O_{26}^{4-}$	0	0	0.0107	0.0082	0.0078	0
$(C_6H_5P)_2Mo_5O_{21}^{4-}$	0.300	0.1103	0.0762	0.0608	0.0518	0
$(C_6H_5P)Mo_6O_{21}(OH_2)_5^{2-}$	0	0	0	0.1190	0.1965	0
$(C_6H_5P)Mo_7O_{25}(OH_2)^{4-}$	0	0.0795	0.1476	0.0595	0	0

[a] $[MoO_4^{2-}] = 0.5025$ mol·dm^{-3}.

contains the complexes MoO_4^{2-} and $Mo_7O_{24}^{6-}$. The structure parameters of the $Mo_7O_{24}^{6-}$ and $Mo_8O_{26}^{4-}$ complexes, present in solutions II and VI and in solutions III−V, respectively, were taken from studies in the solid state.[8,9] As already pointed out, the situation was further complicated by the fact that the presence of two of the species, Mo$_6$-PhP and Mo$_7$PhP, has only been established in equilibrium analysis investigations.[3]

Quantitative ^{31}P NMR measurements performed on solutions II−V, both before and after the LAXS investigation, confirmed that the concentrations of the species present are in good agreement with the distribution diagram (Figure 1) and no change in the complex distribution took place during the collection of LAXS data. However, there is an uncertainty concerning the distribution between the Mo$_7$-PhP and Mo$_6$PhP species (thick dashed line) because it is not possible from the NMR spectra to distinguish between these two species of different nuclearities owing to rapid exchange on the NMR time scale. Moreover, the NMR-measurements on the concentrated LAXS solutions indicate small amounts of an additional molybdophenylphosphonate species in acidic solutions III−V. This new and broad peak in the NMR spectra probably represents species of higher nuclearity than the species found in the equilibrium study.

Large-Angle X-ray Scattering Measurements. A large-angle $\theta-\theta$ diffractometer, described elsewhere,[10] was used to measure the Ag Kα ($\lambda = 0.5609$ Å) X-ray scattering from the free surface of each solution. The scattered intensities were measured by means of a scintillation counter at ca. 440 discrete θ values in the step scan mode with $\Delta\theta$ intervals of 0.10° for $1 < \theta < 30$° and 0.25° for $30 < \theta < 65$° of the scattering angle 2θ. At least 40 000 counts were accumulated twice for each θ value, corresponding to a statistical error of 0.5%. The reflections from a gold plate were used to calibrate the 2θ scattering angle of the goniometer. A vertical Soller slit followed by a horizontal 1° divergence slit was used to limit the primary beam from the X-ray source, except for small scattering angles, $\theta < 10$°, where smaller slits, $^1/_{12}$ and $^1/_4$°, were necessary. Bragg−Brentano semifocusing geometry was used with a distance between the line focus and the center of the sample of 16.5 cm. After the sample, a scatter slit having twice the size of the divergence slit was followed by a 0.2 mm focal slit (0.1 mm for the $^1/_{12}$ and $^1/_4$° divergence slits). A Johansson-type[11] focusing LiF monochromator was used to eliminate fluorescence and to partially discriminate against Compton scattering from the sample. A PC-based multichannel scaling board[12] with further energy discrimination against background radiation and electronic noise reduced the background count rate to less than 0.5 cps. The compositions, densities, absorption coefficients, and stoichiometric unit volumes of the solutions studied are summarized in Table 1, and their compositions are given in Table 2.

Treatment of LAXS Data. The measured intensities of the solutions were corrected for sample transparencies because of low absorption (see Table 1) and applied to each slit combination.[13] The experimental intensities from different scans were scaled to a common basis, corrected for polarization, and normalized to a stoichiometric unit volume corresponding to one molybdenum atom using the KURVLR pro-

gram.[10,14] The reduced structure-dependent intensities, $i(s)$, were obtained after subtraction of the sum of the calculated structure-independent scatterings.[15] The incoherent part, i.e., the Compton scattering,[15] was corrected for recoil effects in the form appropriate for a scintillation counter[16] and multiplied by an instrumental function describing the fraction passing through the LiF monochromator, ca. 0.11 for $s > 10$ Å^{-1}. The coherent part of the structure-independent scattering[15] was calculated using scattering factors, $f(s)$, for the neutral atoms, including their anomalous dispersion corrections, $\Delta f'$ and $\Delta f''$.[17] The most important formulas used in the data treatment and the calculation of reduced intensities from molecular models are given elsewhere.[5] Least-squares refinements of some of the model parameters were carried out by using the STEPLR program.[18]

Analysis of Data and Discussion

To describe the solution structures of the complexes formed in the molybdophenylphosphonate systems in aqueous solution, several models were tested. Because of the complexity of the systems and the complex structures of the heteropolymolybdate species formed, detailed knowledge of their structures or structural information from related species is required in the modeling process. Furthermore, assumptions were made that the intermolecular interactions of reference solutions I and VI and of an aqueous solution of lithium molybdate(VI) reported elsewhere[7] could be used as an approximation for corresponding interactions in the solutions containing complexes of previously undetermined structures (solutions II−V). Since the number of parameters possible to include in the refinement process is limited, the parameters obtained in previous studies were fixed in subsequent calculations of the complexes with known structure. The models used in the calculations were mainly based on various solid-state structures. If no such structures were available, related structures had to be applied when structures of certain molybdophenylphosphonate species were lacking. The concentrations of the species present in the models for different solutions are compiled in Table 2. The concentrations of lithium were based on the initial amounts of lithium molybdate dissolved. The concentrations of water were calculated from density determinations of the solutions and are given in Table 1.

The contribution to the total scattering from lithium is always very small, and the accuracy of the structural parameters of the hydrated lithium ion is therefore low. The best fit of an aqueous solution of lithium molybdate(VI) was obtained with the hydrated lithium ion being tetrahedral and an Li−O bond distance of 1.96(5) Å. The Mo−O bond distance in a hydrated molybdate ion is 1.795(5) Å, with an Mo···O$_{II}$ distance to the water oxygens hydrating the molybdate ion at ca. 4.0 Å.[7] The Mo−O bond distance is significantly elongated in aqueous solution, owing to hydrogen bond formation upon hydration, in comparison with an average Mo−O distance of 1.773 Å in the solid state, where rarely more than one or two molybdate oxygens are hydrogen-bonded.[19]

Solutions II−V contain, besides the hydrated lithium ions and the Mo$_5$(PhP)$_2$ complexes, at least one isopolymolybdate ion and molybdophenylphosphonate ions of different nucleari-

(10) Stålhandske, C. M. V.; Persson, I.; Sandström, M.; Kamienska-Piotrowitz, E. *Inorg. Chem.* **1998**, *37*, 3174−3182.

(11) Crismatec, Nemours, France.

(12) AccuSpec FMS Masterboard, Canberra, Nuclear Data Systems, Schaumburg, IL.

(13) Milberg, M. E. *J. Appl. Phys.* **1958**, *29*, 64−65.

(14) Johansson, G.; Sandström, M. *Chem. Scr.* **1973**, *4*, 195−198 and references therein.

(15) Cromer, D. T.; Mann, J. B. *J. Chem. Phys.* **1967**, *47*, 1892−1893. Cromer, D. T. *J. Chem. Phys.* **1969**, *50*, 4857−4859.
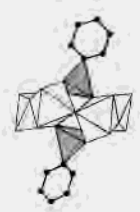
(16) Dwiggins, C. W., Jr.; Park, D. A. *Acta Crystallogr., Sect. A* **1971**, *27*, 264−272.

(17) *International Tables of Crystallography*; Wilson, A. J. C., Ed.; Kluwer Academic Publishers: Dordrecht, The Netherlands, 1995; Vol. C.

(18) Molund, M.; Persson, I. *Chem. Scr.* **1985**, 25, 197.

(19) Matsumoto, K. Y.; Kobayashi, A.; Sasaki, Y. *Bull. Chem. Soc. Jpn.* **1975**, *43*, 1009−1013.

Table 3. Selected Distances, *d*, Atomic Displacement Factors, *l*, and Numbers of Distances, *n*, Used in the Calculation of Shape Functions (Water Oxygens Represented as Open Rings in Structures)

Complex	Interaction	*d*/Å	*l*/Å	*n*	Structure
MoO_4^{2-} [a]	Mo–O	1.795	0.110	4	
	O···O	2.931	0.126	6	
$Mo_7O_{24}^{6-}$ [b]	Mo···Mo	3.23, 3.42, 4.17, 5.70	0.063	6, 6, 2, 4	
	Mo–O	1.72, 1.93, 2.27	0.126	12, 14, 6	
	O···O	2.5–2.9, 3.7–3.9	0.155	68, 14	
$Mo_8O_{26}^{4-}$ [c]	Mo···Mo	3.24, 3.47, 4.59, 5.69	0.063	8, 8, 4, 6	
	Mo–O	1.71, 1.94, 2.32	0.126	16, 16, 12	
	O···O	2.5–2.9, 3.7–3.8	0.155	72, 20	
$(C_6H_5P)_2Mo_5O_{21}^{4-}$ [d]	Mo···Mo	3.45, 5.55	0.063	5, 5	
	Mo···P	3.46	0.063	10	
	P···P	3.74	0.063	1	
	Mo–O	1.71, 1.93, 2.31	0.126	10, 10, 10	
	P–O	1.53	0.126	6	
	O···O	2.5–3.0, 3.6–3.7	0.155	60, 8	
$(C_6H_5P)Mo_6O_{21}(OH_2)_5^{2-}$ [e]	Mo···Mo	3.35, 3.61, 5.71, 6.00	0.063	3, 3, 3, 3	
	Mo···P	3.50	0.063	6	
	Mo–O	1.71, 1.91, 2.30	0.126	12, 12, 12	
	P–O	1.54	0.126	3	
	O···O	2.5–2.9, 3.6–3.7	0.155	64, 8	
$(C_6H_5P)Mo_7O_{25}(OH_2)^{4-}$ [f]	Mo···Mo	3.33, 3.64, 5.63, 6.06	0.063	4, 8, 4, 3	
	Mo···P	3.56, 3.77, 5.22	0.063	4, 1, 2	
	Mo–O	1.70, 1.91, 2.30	0.126	16, 12, 12	
	P–O	1.54	0.126	3	
	O···O	2.5–2.9, 3.4–3.9	0.155	74, 22	
$Li(OH_2)_4^+$ [a]	Li–O	1.965	0.126	4	
	O···O	3.209	0.155	6	
H_2O	O···O	2.87	0.283	1	

[a] Ref. 7, [b] Ref. 8, [c] Ref. 9, [d] Ref. 4, [e] Ref. 23, [f] Ref. 22.

ties. The temperature factor coefficients of the atomic positions in the isopolymolybdate and molybdophenylphosphonate ions were given values similar to those found in $Mo_5(PhP)_2$. Several different models of the molybdophenylphosphonate complexes were tested. These models were derived from other similar complexes in the solid state (see below), as the molybdophenylphosphonate complexes have not yet been structurally characterized.

Concentrations for the various complexes derived from potentiometric and NMR spectroscopic measurements, summarized in Table 2, wee used in calculations of theoretical RDFs. Incorrect models and incorrect combinations of models always cause fairly large irregularities in the differences between the experimental and theoretical RDFs. The RDFs, the individual contributions from different complexes, and the theoretical reduced intensity functions for the best set of models for solutions I−VI are given in Figures 3−8, respectively.

A comparison between the experimental radial functions of solutions I−V (Figures 3−7) shows that the characteristic peak at 5.6 Å is gradually reduced. This peak is assumed to be associated with the diagonal Mo···Mo distances in the five-

membered ring of the $Mo_5(PhP)_2$ complex, whose structure in the solid state is reported.[4] Further support of the validity of this assumption is found in the distribution diagram in Figure 2, where it can be seen that the concentration of the $Mo_5(PhP)_2$ species is reduced when pH decreases. Since solution I contains only the $Mo_5(PhP)_2$ species and there is good agreement between model and experimental curves of this solution (Figure 3), it is concluded that the structure of $Mo_5(PhP)_2$ observed in solid state (Figure 9a) remains in aqueous solution. The resulting difference curve is smooth, and the broad feature between 3 and 5.5 Å is probably associated with randomly distributed distances in the remaining aqueous bulk and between the anions and hydrating water molecules.

The $Mo_5(PhP)_2$ structure, with the appropriate concentration (see Table 2), was subsequently used to describe the contribution from the $Mo_5(PhP)_2$ species in the distribution functions for solutions II−V. The solid-state structure of the $Mo_7O_{24}^{6-}$ complex[8] (Figure 9b) was tested in solution VI, and it was found that a very good fit was obtained (see Figure 8), showing that the structure of the $Mo_7O_{24}^{6-}$ complex is maintained in aqueous solution. This structure was therefore used as a model in solution

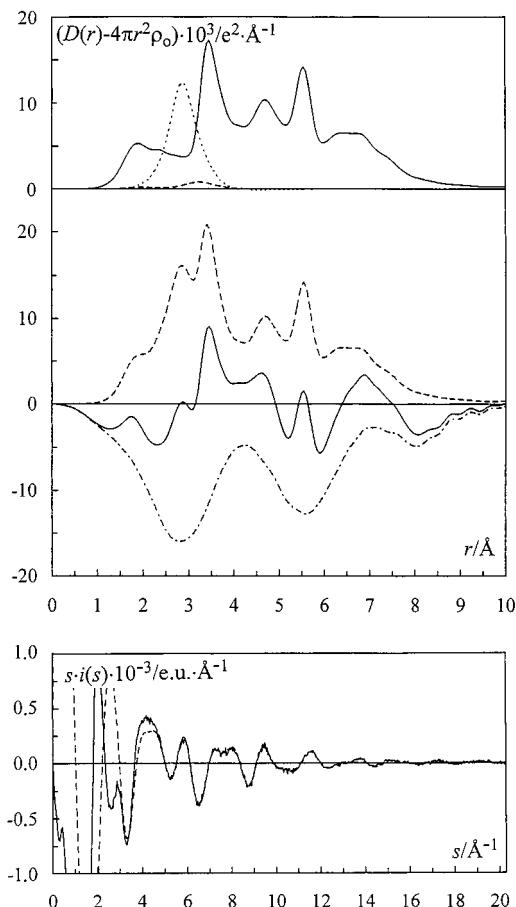**Figure 3.** Experimental and theoretical plots for solution I. Top panel, upper part, shows the separate model contributions: H_2O (<3 Å), dotted line; $Li(OH_2)_4^+$, dashed line; $(C_6H_5P)_2Mo_5O_{21}^{4-}$, solid line. Top panel, lower part, shows the experimental radial distribution function, $D(r) - 4\pi r^2\rho_0$ (solid line), sum of calculated peak shapes (dashed line), and the difference between the experimental and model functions (dashed–dotted line). Bottom panel shows the reduced LAXS intensity function, $s\cdot i(s)$ (solid line), and calculated model contributions (dashed line).

Figure 4. Experimental and theoretical plots for solution II. Top panel, upper part, shows the separate model contributions: H_2O (<3 Å), thin dotted line; $Li(OH_2)_4^+$, dashed line; $(C_6H_5P)_2Mo_5O_{21}^{4-}$, solid line; $Mo_7O_{24}^{6-}$, thick dotted line; $(C_6H_5P)Mo_7O_{25}(OH_2)^{4-}$, dashed–double-dotted line. Top panel, lower part, shows the experimental radial distribution function, $D(r) - 4\pi r^2\rho_0$ (solid line), sum of calculated peak shapes (dashed line), and the difference between the experimental and model functions (dashed–dotted line). Bottom panel shows the reduced LAXS intensity function, $s\cdot i(s)$ (solid line), and calculated model contributions (dashed line).

II. The solid-state structure parameters of the $Mo_8O_{26}^{4-}$ complex[9] (Figure 9c) were applied as models in solutions III–V. These models were used as fixed parameters for solutions II–V to give the contributions of these complexes (see Figure 2). The remaining peaks and shoulders should then reflect the contributions from the Mo_7PhP and/or Mo_6PhP complexes. As already mentioned, the structures of these complexes were not previously known from solid-state investigations. A major goal of this investigation was therefore to try to elucidate the structures of these complexes.

The first model tested for the Mo_7PhP and Mo_6PhP complexes was based on the $(AsO_4)_2Mo_6O_{18}^{6-}$ structure,[20] where the two AsO_4 tetrahedra are capped on each side of a planar six-membered ring of edge-sharing MoO_6 octahedra (Figure 9d). To adapt this structure to the Mo_7PhP complex, the two AsO_4 tetrahedra were replaced by one CPO_3 group and one MoO_4 tetrahedron. The model of the Mo_6PhP species was obtained by replacing one AsO_4 tetrahedron by one CPO_3 group while the other AsO_4 tetrahedron was removed. Any satisfactory fit of the experimental pattern could however not be obtained with this model.
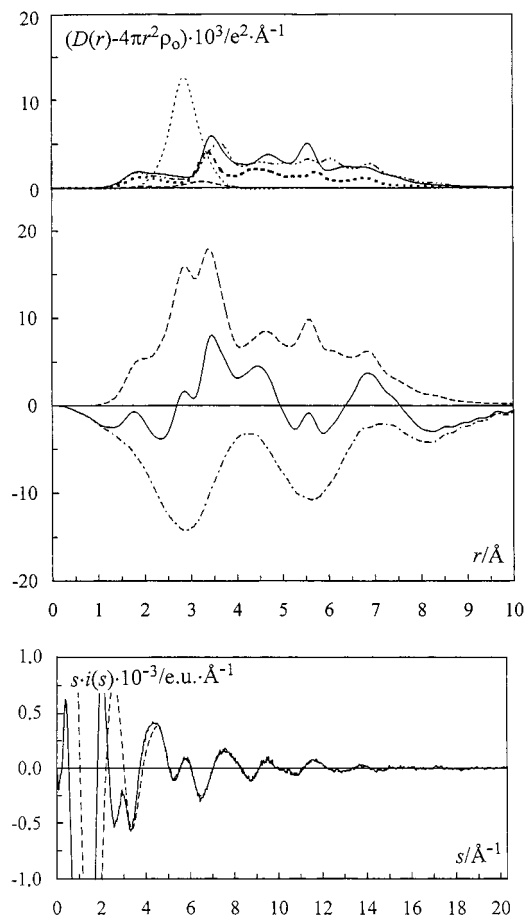
In a second model, the Mo_6PhP complex was based on the $(CH_3AsO_3)Mo_6O_{18}(H_2O)_6^{2-}$ structure,[21] which consists of a six-membered ring of alternate corner- and edge-sharing MoO_6 octahedra where the CH_3AsO_3 group is coordinated to the edge-sharing octahedra (Figure 9e). The CH_3AsO_3 group was then replaced by a CH_3PO_3 group to obtain the Mo_6PhP species. The two models based on the $(AsO_4)_2Mo_6O_{18}^{6-}$ and CH_3AsO_3-$Mo_6O_{18}(H_2O)_6^{2-}$ structures are highly symmetrical with distinct $Mo\cdots Mo$ distances. This implies few and sharp peaks in the radial distribution function, which definitely could not explain the experimental data.

A third model based on the $(C_6H_5AsO_3)_2Mo_6O_{18}(H_2O)^{4-}$ structure[22] (denoted model A) was also tested. This anion has one group of four edge-sharing MoO_6 octahedra (Mo4) and another group of two face-sharing MoO_6 octahedra (Mo2). The two groups of MoO_6 octahedra are connected by sharing corners, forming a bent unsymmetrical six-membered ring. The two $C_6H_5AsO_3$ groups are connected on each side of the ring in two fashions: one group is coordinated only to the Mo4 group whereas the other group is coordinated both to the Mo4 group and to the Mo2 group on the opposite side of the ring. This leads to two constructions of each of the two complexes, as the two $C_6H_5AsO_3$ groups are replaced by (1) one $C_6H_5PO_3$ group

(20) Hedman, B. *Acta Crystallogr.*, *Sect. B* **1980**, *36*, 2241–2246.
(21) Matsumoto, K. Y. *Bull. Chem. Soc. Jpn.* **1979**, *52*, 3284–3291.
(22) Matsumoto, K. Y. *Bull. Chem. Soc. Jpn.* **1978**, *51*, 492–498.
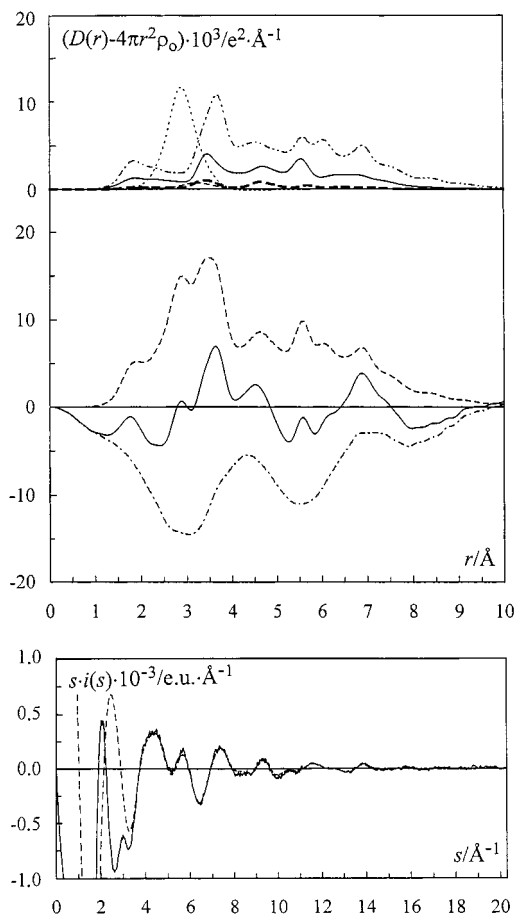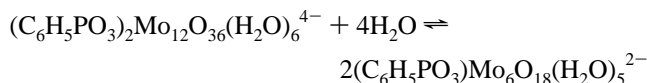
Figure 5. Experimental and theoretical plots for solution III. Top panel, upper part, shows the separate model contributions: H_2O (<3 Å), dotted line; $Li(OH_2)_4^+$, thin dashed line; $(C_6H_5P)_2Mo_5O_{21}^{4-}$, solid line; $Mo_8O_{26}^{4-}$, thick dashed line; $(C_6H_5P)Mo_7O_{25}(OH_2)^{4-}$, dashed−double-dotted line. Top panel, lower part, shows the experimental radial distribution function, $D(r) - 4\pi r^2 \rho_0$ (solid line), sum of calculated peak shapes (dashed line), and the difference between the experimental and model functions (dashed−dotted line). Bottom panel shows the reduced LAXS intensity function, $s \cdot i(s)$ (solid line), and calculated model contributions (dashed line).
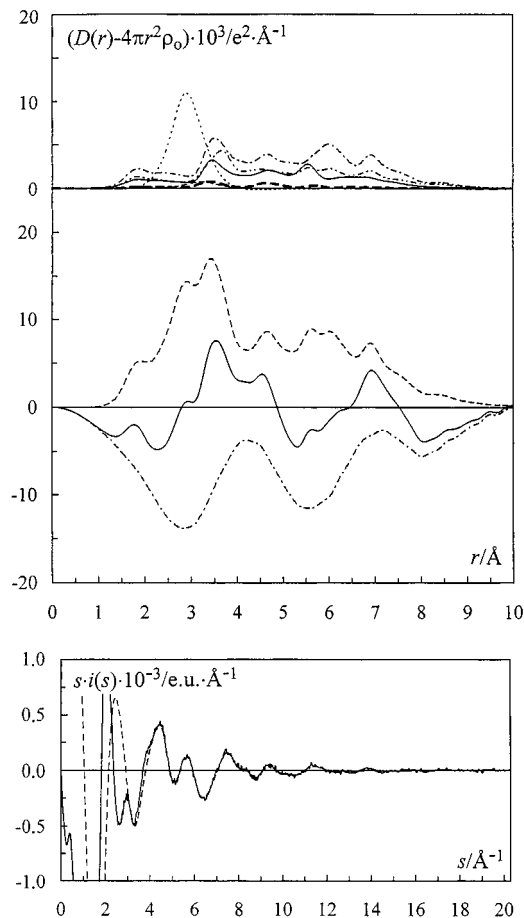

Figure 6. Experimental and theoretical plots for solution IV. Top panel, upper part, shows the separate model contributions: H_2O (<3 Å), dotted line; $Li(OH_2)_4^+$, thin dashed line; $(C_6H_5P)_2Mo_5O_{21}^{4-}$, solid line; $Mo_8O_{26}^{4-}$, thick dashed line; $(C_6H_5P)Mo_7O_{25}(OH_2)^{4-}$, dashed−double-dotted line; $(C_6H_5P)Mo_6O_{21}(OH_2)_5^{2-}$, dashed−dotted line. Top panel, lower part, shows the experimental radial distribution function, $D(r) - 4\pi r^2 \rho_0$ (solid line), sum of calculated peak shapes (dashed line), and the difference between the experimental and model functions (dashed−dotted line). Bottom panel shows the reduced LAXS intensity function, $s \cdot i(s)$ (solid line), and calculated model contributions (dashed line).

to represent a Mo_6PhP composition and (2) one $C_6H_5PO_3$ group plus one MoO_4 tetrahedron to represent a Mo_7PhP composition. The best model to fit data for the solutions containing Mo_6PhP and Mo_7PhP complexes was obtained when the $C_6H_5PO_3$ group was placed on the crowded side of the ring (Figure 9f), i.e., linked to both the Mo4 and Mo2 groups and not to the other side of the ring (Figure 9g). However, some artifacts, especially for solution V, appeared in the difference curve and $s \cdot i(s)$ curve when the Mo_6PhP complex was modeled.

Recently, a single-crystal X-ray investigation was reported for a trimethylammonium salt containing the $[(C_6H_5PO_3)Mo_6O_{18}-(H_2O)_3]_2^{4-}$ anion[23] (Figure 9h), which consists of two $(C_6H_5-PO_3)Mo_6O_{18}(H_2O)_3$ entities weakly bound to each other. This anion can be regarded as a dimer of these entities according to the equilibrium

$$(C_6H_5PO_3)_2Mo_{12}O_{36}(H_2O)_6^{4-} + 4H_2O \rightleftharpoons$$
$$2(C_6H_5PO_3)Mo_6O_{18}(H_2O)_5^{2-}$$

The $(C_6H_5PO_3)Mo_6O_{18}(H_2O)_5^{2-}$ complex (model B, Figure 9i)

(23) Lyxell, D.-G.; Boström, D.; Hashimoto, M.; Pettersson, L. *Acta Crystallogr., Sect. B* **1998**, *54*, 424−430.

has a bent six-membered ring of MoO_6 octahedra similar to the complex shown in Figure 9f (model A) except that the group of two MoO_6 octahedra (Mo2 group) is edge-shared instead of face-shared. The $C_6H_5PO_3$ group is coordinated as in model A, i.e., attached to the crowded side of the 6-ring; see Figure 9f,i. This Mo_6PhP model (model B) gives a slightly better fit to the experimental data than model A in solution V but a slightly poorer fit to data in solutions II and III when an MoO_4 tetrahedron is attached to the six-membered ring in model B. The mixture of these two models fits the data very well in solution IV, which contains the complexes Mo_6PhP and Mo_7-PhP, as seen in the distribution diagrams (Figures 1 and 2).

An explanation may be that the six-membered ring in model A can coordinate an MoO_4 tetrahedron to three oxygen atoms in the Mo4 group with an average $O \cdots O$ distance of 2.89 Å. In this model, the $C_6H_5AsO_3$ group has an $O \cdots O$ average distance of 2.77 Å and only a small adjustment is necessary to replace it with an MoO_4 tetrahedron. On the other hand, in model B, it is impossible to coordinate an MoO_4 tetrahedron to the six-membered ring opposite the $C_6H_5PO_3$ group because the distances between the three connecting oxygen atoms in the Mo4 group are too long, caused by the edge-sharing MoO_6
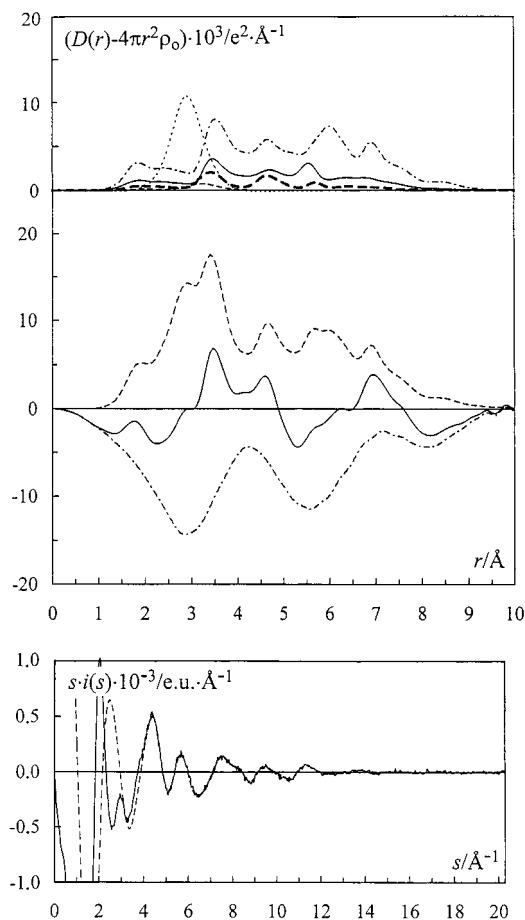
Figure 7. Experimental and theoretical plots for solution V. Top panel, upper part, shows the separate model contributions: H_2O (<3 Å), dotted line; $Li(OH_2)_4^+$, thin dashed line; $(C_6H_5P)_2Mo_5O_{21}^{4-}$, solid line; $Mo_8O_{26}^{4-}$, thick dashed line; $(C_6H_5P)Mo_6O_{21}(OH_2)_5^{2-}$, dashed−dotted line. Top panel, lower part, shows the experimental radial distribution function, $D(r) - 4\pi r^2\rho_0$ (solid line), sum of calculated peak shapes (dashed line), and the difference between the experimental and model functions (dashed−dotted line). Bottom panel shows the reduced LAXS intensity function, $s\cdot i(s)$ (solid line), and calculated model contributions (dashed line).

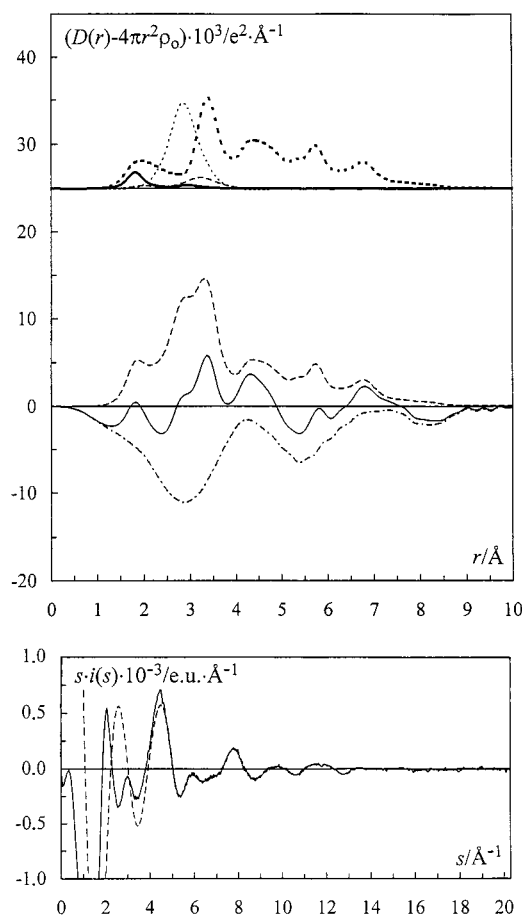**Figure 8.** Experimental and theoretical plots for solution VI. Top panel, upper part, shows the separate model contributions: H_2O (<3 Å), thin dotted line; $Li(OH_2)_4^+$, dashed line; MoO_4^{2-}, solid line; $Mo_7O_{24}^{6-}$, thick dotted line. Top panel, lower part, shows the experimental radial distribution function, $D(r) - 4\pi r^2\rho_0$ (solid line), sum of calculated peak shapes (dashed line), and the difference between the experimental and model functions (dashed−dotted line). Bottom panel shows the reduced LAXS intensity function, $s\cdot i(s)$ (solid line), and calculated model contributions (dashed line).

octahedra in the Mo2 group. The O···O distances are in the range 3.04−3.48 Å and consequently are too long to coordinate to molybdenum. In model B, with two edge-shared octahedra, the distances between the oxygen atoms in the $C_6H_5PO_3$ group are in the range 2.50−2.54 Å and it is also possible to connect a $C_6H_5PO_3$ group to a face-shared Mo2 group as in model A because of its flexibility. After the contribution of identified species from the RDFs of solutions II and V, the remaining contribution comes from the Mo_7PhP and Mo_6PhP species, as can be seen in Figure 2. The corresponding radial distribution curves show a peak at 4.7 Å for solution V which is missing for solution II. The conclusion to be made from this observation is that this peak is associated with the Mo_6PhP complex and can only be explained with the structure of model B. The Mo_7-PhP complex is then associated with the structure of model A.

The difference curves calculated for solutions I−VI show similar shapes, indicating that the remaining bulk structures are almost the same for these solutions (Figures 3−8). Since the various anions have similar sizes and charges, the water−anion, anion−anion and long water−water interactions should be comparable. However, the RDF from solution II has a minor peak at ∼4.4 Å which does not appear in the RDFs of the other PhP-containing solutions and causes a peak in the corresponding

background curve as a result of an insufficient model. It can be seen from the Mo_7PhP distribution in Figure 2 that Mo_7PhP^{4-} is the predominant species in solution III, whereas Mo_7PhP^{5-} predominates in solution II. Model A, which fits well to solution III, has one water oxygen as a face-sharing atom in the Mo2 group of the MoO_6 octahedra (Figure 9f). In this structure the $Mo-OH_2$ distances in the group are elongated, causing a repulsion of the MoO_4^{2-} tetrahedron which is attached to the Mo4 group. A deprotonation of the coodinated water molecule would probably shorten these distances somewhat and probably give a better fit to the experimental data. However, the very small deviation in the background curve for solution II indicates that the model used can in principle be considered to explain the experimental data.

Concluding Remarks

The previous speciation study of the aqueous molybdophenylphosphonate system was performed in an ionic medium of 0.600 mol·dm^{-3} sodium chloride.[3] With such a weak ionic medium, it is not possible to prepare solutions with the high molybdenum concentration needed for an LAXS investigation. When the molybdenum concentration is increased in a sodium chloride medium, precipitation occurs in acidic solution. However, replacing the sodium ions by lithium ions can increase the solubility, making LAXS studies possible. Despite the
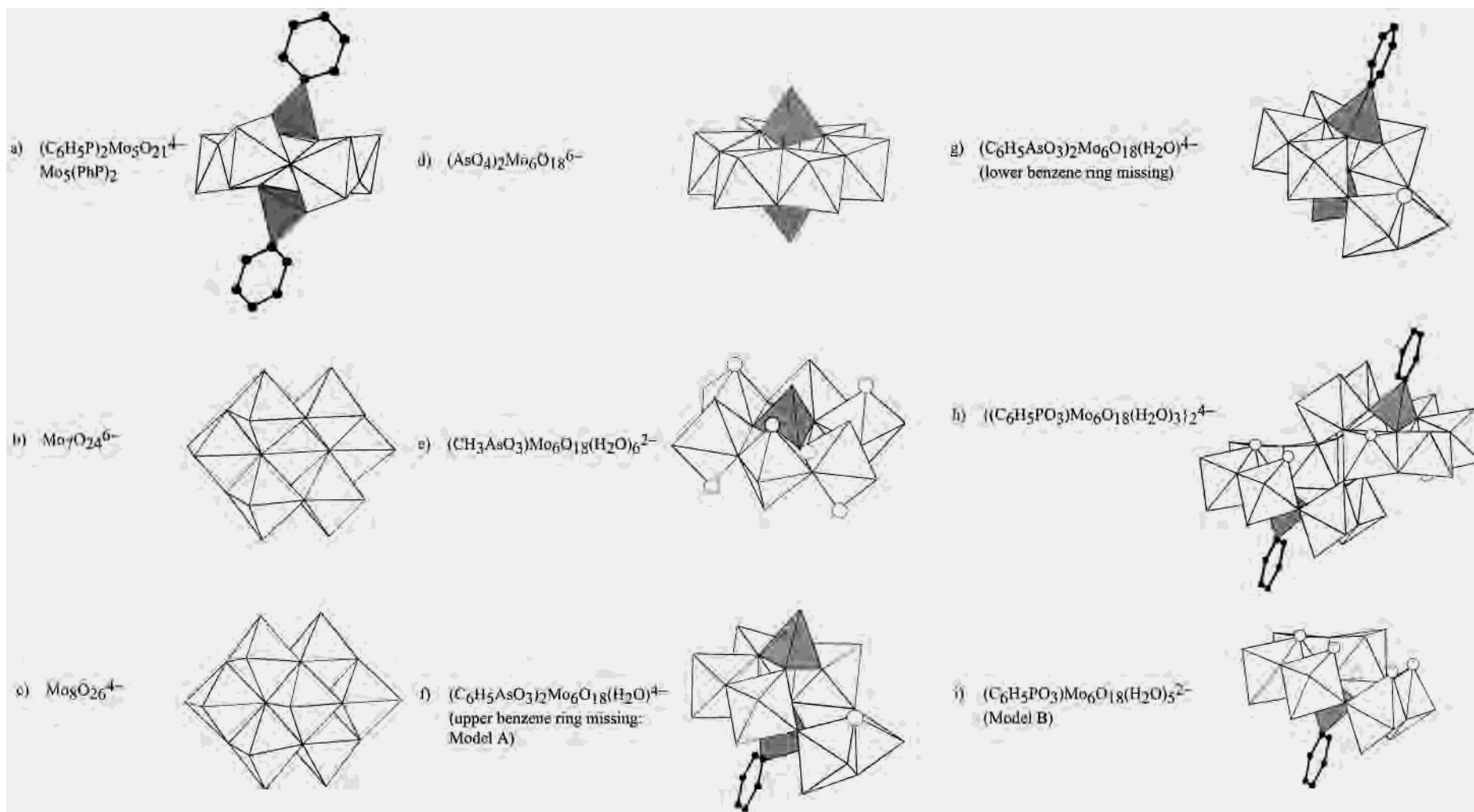
Figure 9. Polyhedral representations of species used in the model calculations.

differences in the medium backgrounds, our LAXS studies on concentrated molybdophenylphosphonate solutions ($C_{Mo} = 1.50$ mol·dm^{-3}) in an LiCl medium are in agreement with the speciations found in the potentiometric and ^{31}P NMR studies on solutions with $C_{Mo} \leq 0.080$ mol·dm^{-3}.[3]

The main purpose of the present study was to determine the aqueous structures of the complexes formed in the system and to understand why two of the species with different nuclearities are in rapid exchange on the ^{31}P NMR time scale. The close correlation between the observed and calculated *s·i(s)* functions confirms that the structure of the discrete anion $(C_6H_5P)_2Mo_5O_{21}{}^{4-}$ ($Mo_5(PhP)_2$) and that of the monomic unit Mo_6PhP, discernible in the dimeric $[(C_6H_5PO_3)Mo_6O_{18}(H_2O)_3]_2{}^{4-}$ anion, both found in single-crystal X-ray determinations,[4,23] are present in aqueous solution. Modeling of the Mo_7PhP complex, based on the $(C_6H_5AsO_3)_2Mo_6O_{18}(H_2O)^{4-}$ structure,[22] also confirms the relevance of the earlier proposed structure,[3] and it was even

possible to localize the water oxygen site in the structure due to the lengthening of the $Mo_2\cdots Mo$ distances. The similar structural features of the Mo_6PhP complex and the two Mo_7-PhP complexes explain why the three species are in rapid exchange on the ^{31}P NMR time scale. This study has shown how powerful the LAXS technique is even in this complex molybdophenylphosphonate system, where species having similar structures are formed. Without clues from solid-state structures it is, however, impossible to fully elucidate the aqueous structures in such a complicated system.

IC000711Y